HETEROGENEITY IN THE SIZE OF THE APICAL SURFACE OF CORTICAL PROGENITORS

Caroline Badouel[1], Christophe Audouard[1] and Alice Davy[1*]

[1] Molecular, Cellular and Developmental Biology Unit (MCD), Centre de Biologie Intégrative (CBI), Université de Toulouse, CNRS, UPS, 118 route de Narbonne, 31062 Toulouse, France.

*Correspondance : Alice Davy, MCD-CBI, 118 route de Narbonne, Bat 4R4, 31062 Toulouse France (alice.davy@univ-tlse3.fr). ORCID **:** 0000-0003-2134-4526.

Keywords : ephrin ; neural progenitors ; mechanics ; morphogenesis ; mouse

ABSTRACT

The apical surface of epithelial cells is highly specialized, it is important for morphogenetic processes that are essential to shape organs and tissues and it plays a role in morphogen and growth factor signaling. Apical progenitors in the mammalian neocortex are pseudoepithelial cells whose apical surface lines the ventricle. Whether changes in their apical surface sizes are important for cortical morphogenesis and/or other aspects of neocortex development after neurulation has not been thoroughly addressed. Here we show that apical progenitors are heterogeneous with respect to their apical surface area. In *Efnb1* mutants, the size of the apical surface is modified and this correlates with discrete alterations of tissue organization without impacting proliferation or differentiation. Altogether, our data reveal heterogeneity in apical progenitors AS area in the developing neocortex and shows a role for Ephrin B1 in controlling AS size. Our study also indicates that changes in AS size does not have strong repercussion on apical progenitor behavior.

INTRODUCTION

Epithelial cells or cells with epithelial features are widespread in metazoans (Tyler, 2003). These cells are characterized by a polarized morphology with distinct basolateral and apical membranes and a tight cell-to-cell adhesion. The apical membrane or apical surface (AS) of epithelial cells is highly specialized, it harbors different organelles depending on the epithelial cell type, such as microvilli, a primary cilium or multiple cilia. Because numerous growth factor receptors, transporters and channels are enriched apically in epithelial cells, the AS plays an important role in sensing environmental cues. In addition, the AS participates in organ morphogenesis during embryonic development. Indeed, it has been shown that constriction of the AS is a key step in epithelium folding and invagination (Martin et al., 2009). While modifications in AS area have been tightly linked to morphogenesis of epithelial sheets in different contexts (Sawyer et al., 2010), whether and how changes in AS area might also impact complex tissues has not been investigated thoroughly.

The developing neocortex, the dorsal part of the mammalian forebrain, is a complex tissue elaborated from a pseudo-epithelial sheet. Indeed, the neocortex is composed of a diversity of cells that originate from an initial pool of pseudo-epithelial neural progenitors also called apical progenitors. Apical progenitors are polarized, elongated cells, whose apical endfeet line the ventricular surface of the neocortex while their basal processes extend towards the pial surface. Apical progenitors either divide symmetrically, thereby amplifying their population, or asymmetrically to produce other cell types including intermediate progenitors and neurons (Miyata et al., 2004; Noctor et al., 2004). As soon as they are generated, intermediate progenitors and neurons detach from the apical surface of the tissue and migrate basally, such that the apical (ventricular) surface of the tissue is formed exclusively by the tiling of apical progenitors AS. One special feature of the neuroepithelium is the existence of interkinetic nuclear migration (IKNM) whereby apical progenitors' nuclei migrate during the cell cycle from an apical location in mitosis to a basal location in S-phase (Sauer and Walker, 1959). Due to IKNM, the cytoarchitecture of apical progenitors AS changes over the cell cycle, broadening during mitosis

and tightening during the other phases (Nagele and Lee, 1979). As a result of proliferation and differentiation events, reorganization of the ventricular surface occurs constantly to accommodate apical mitosis and delamination events, impacting on tissue integrity and biophysical parameters, as shown for other epithelia (Pinheiro and Bellaïche, 2018).

In addition to these dynamic events, it has been shown that the mean size of AS area changes over the course of development in the mouse neocortex (Nishizawa et al., 2007) and that it differs across brain regions, being smaller in the pallium than in the ganglionic eminence (Nagasaka and Miyata, 2021). Yet, the functionnal significance of these changes is not clear and very little is known on the mechanisms regulating the size of apical progenitors AS.

Ephrin B1 is a member of the Eph:Ephrin family which is involved in promoting cell adhesion or cell repulsion depending on the cellular context (Cayuso et al., 2015; Fagotto et al., 2014). In a previous set of experiments we reported that a fraction of *Efnb1* mouse mutant embryos exhibit neural tube closure defects and microfolding of the ventricular surface, which we attributed to a loss of progenitor apical adhesion (Arvanitis et al., 2013). Here we used en-face fixed and live imaging to quantitatively characterize the size of apical progenitors AS in wild type and *Efnb1* mutant contexts. First, we show that apical progenitors in a wild type context are heterogeneous with respect to their AS areas and that this heterogeneity is not only linked to IKNM. We then use genetic tools to perturb Ephrin B1 expression and show that it modifies AS area without impacting on apical progenitors proliferation or differentiation. Moreover, mosaic loss of Ephrin B1 expression reveals strong non cell-autonomous mechanical feedback on AS size.

RESULTS

En-face analysis of cortical progenitors AS

To visualize the AS of apical progenitors, we exposed the ventricular surface by dissecting out the neocortex as illustrated in Figure 1A. Cortical explants were then stained with an F-actin probe, to

delineate individual AS, and segmented to measure their sizes (Fig. 1B). Quantification of apical areas revealed that the average apical domain is 4.4μm^2 (+/- 0.42 μm^2), with a median of 3.8 μm^2 at E13.5. Analysis of size distribution showed large variation in apical area sizes, with around 15% of very small AS (<2 μm^2) and around 20% of larger AS (>6 μm^2) (Fig. 1C). A previous systemic survey of AS area in the developing cortex indicated that apical surfaces tend to increase in size between E12 to E15 (Nishizawa et al., 2007). Indeed, when we quantified AS areas one day later in development, at E14.5, we observed a shift in size distribution towards bigger AS (Fig. 1D, Average of 5.4μm^2). To ask whether these variations in AS sizes are intrinsic to the developing tissue, we cultured embryonic cortical explants in vitro and performed live imaging with an en-face view of the ventricular wall. We validated our culture conditions using an H2B reporter mouse line to visualize progenitor nuclei. We confirmed that apical progenitors divide properly, with intact interkinetic nuclear migration and cytokinesis events (Movie 1 and data not shown). Development of apical domains were followed for 14hrs (Movie 2), and each image was segmented (Movies 3) to quantify epithelial growth dynamics. These movies revealed an increase in AS size during the 14hrs time lapse (Fig. 1D-F: 5.4μm^2 +/- 0.6 μm^2 at T0 versus 6.21μm^2 +/- 0.4 μm^2 after 15hrs, p=0.019*), indicating that the increase in AS size is intrinsic to the tissue. We then characterized individual AS, chosen among those which did not go through cytokinesis during this time window, and followed their size (Movie 4 and Fig. 2A, B). This analysis revealed that surface areas are relatively stable, with big AS tending to stay big and small ones, small (Movie 4 and Fig. 2C; 50 AS analyzed). A measure of size variation from T0 showed that the standard deviation never exceeds 50% of the initial size, confirming stability of AS (Fig. 2D). This data suggests that the increase in average AS area over time is driven by an increase in the proportion of larger AS and not by an increase in the size of all AS. Next, we wondered if heterogeneity in AS sizes could be linked to specific phases of the cell cycle or to mitosis. Apical progenitors' nuclei move to the ventricular surface to divide, which is accompanied by an enlargement of the apical surface. We measured the AS of cells before mitosis and their corresponding daughter cells after cytokinesis for more than 20 dividing progenitors (Fig. 2E, F and Movie 5). Sizes were plotted with T0 representing the time at which 2

daughter cells are first visible (Fig. 2F). This revealed that, indeed, AS are larger prior to division and AS of daughter cells are on average half that size (Fig. 2F). However, the persisting heterogeneity of AS sizes throughout cell division (5-20μm^2 before division and 1-12 μm^2 after division) suggests that this heterogeneity is not the reflection of cell cycle progression.

Mutations in *Efnb1* modifies AS sizes distributions

We previously reported that ephrin B1 is enriched at the apical surface of apical progenitors and that *Efnb1* mutant embryos exhibit defects at the ventricular surface such as microfolding and basal displacement of nuclei (Arvanitis et al., 2013). Because Eph : Ephrin B1 signaling has been shown to promote actomyosin accumulation in different contexts, we hypothesized that it could control junctional tension between AP and potentially impact on AS size. To investigate this hypothesis, we measured junctional tension using laser ablation in wild type and *Efnb1*$^{-/-}$ mutant contexts (Fig. 3A-C and Movies 6,7). Strikingly, recoil distance after ablation was on average twice longer in *Efnb1*$^{-/-}$ mutants compared to wild-type controls (Fig. 3B, initial recoil of 0.045 vs 0.22 in wildtype). When looking at the individual data at 60 seconds after the ablation, we noticed that the distance of recoil is not uniformly increased for all *Efnb1*$^{-/-}$ ablated junctions. Instead, the range of recoiled distances is higher in *Efnb1*$^{-/-}$ mutants compared to wildtype with a fraction of measurements that are higher than in wildtype whereas many recoil distances are similar in both genotypes (Fig. 3C). To assess whether this difference in junctional tension correlates with differences in AS size, we analyzed AS of apical progenitors in *Efnb1* heterozygote and null contexts (Fig. 3D). We observed an increased average AS size in embryos completely lacking Ephrin B1 (*Efnb1*$^{-/-}$) compared to wild-type siblings (Fig. 3E, F). Quantification at population level revealed that *Efnb1*$^{-/-}$ and *Efnb1*$^{+/-}$ mutants show different size distributions compared to wild-type control with an increase in the proportion of large AS (Fig. 3G, H). In addition, we also observed an increased proportion of small AS in *Efnb1*$^{+/-}$ mutants (Fig. 3G, H). These results do not support the hypothesis that Ephrin B1 directly modulates apical constriction via the

actomyosin network since increased junctional tension in this scenario should lead to increased constriction and smaller AS size in *Efnb1*$^{-/-}$ embryos. Nevertheless, this data indicates that Ephrin B1 plays a role in junctional tension and in the control of apical progenitors AS size.

Mosaic ephrin B1 expression modifies AS area

To further assess the role of Ephrin B1 on the regulation of AS size, we focused on *Efnb1*$^{+/-}$ heterozygote tissues which showed an unexpected distribution of AS sizes (Fig. 3E-H). One particularity of *Efnb1*$^{+/-}$ heterozygote tissues is that they are mosaic for Ephrin B1 expression. Indeed, *Efnb1* is on the X chromosome and therefore subject to random X-inactivation. Moreover, Ephrin B1 positive and negative cells tend to sort out in development, creating patches of Ephrin B1 negative cells next to positive cells (Compagni et al., 2003; Davy et al., 2004), Fig. 4A). Co-staining of Ephrin B1 and actin in the en-face view revealed a stereotypical spatial organization of patches of cells negative for Ephrin B1 (called B1- patches) surrounded by Ephrin B1 positive cells (Fig.4B). Strikingly, all B1- patches include clusters of cells with very small AS while cells at the periphery display larger AS (Fig. 4B). Quantification at E13.5 showed a gradient in AS sizes from large in the first row outside the patch (B1+) to small at the center of the patch (B1-) (Fig 4C, E). At E13.5, AS have an average size of 2.6 μm^2 at the center of B1- patches, and 9.2 μm^2 in the first row of B1+ compared to 4.4 μm^2 in a wild-type cortex. This stereotypical organization is even more pronounced at E14.5, where the gradient ranges from 4 μm^2 at the patch center to 20 μm^2 at the periphery (compared to 5.4 μm^2 in average in wild-type, Fig. 4D, E). Z-stacks analysis of B1- patches further revealed that more F-actin accumulates at the apical junctions of the cells at the center and F-actin extends more basally, compared to their neighbors (Fig. 4F) consistent with increased apical constriction. Of note, the ventricular surface remains flat throughout the patches indicating that apical constriction is not the main driver of microfolding (Fig. 4G).

It was unexpected to observe that only B1- cells at the center of the patch have a smaller AS but not B1- cells close to the periphery. We also observed that the AS of B1+ cells near the border were systematically larger than average. Taken together, these observations suggested that the modification in AS sizes could be non-autonomous. To test for this, we analyzed patches of B1+ cells surrounded by B1- territories (Fig. 5 A). Quantification showed that these B1+ patches behave similarly to B1- patches, with a similar gradient in AS size at E13.5, from small at the center of the patch (3.7μm^2) to large at the periphery (9.6 μm^2; Fig. 5B, C). Together, these results suggest that quantitative differences in Ephrin B1 expression in neighboring cells lead to an increase in AS size, in both B1+ and B1- cells and that the decrease in AS size at the center of patch is a non-cell-autonomous effect, secondary to the enlargement of AS at the periphery. Strengthening this hypothesis, we noticed that when 2 very large territories of B1+ and B1- cells are juxtaposed, the enlargement at the border is visible but no clear decrease in AS size is observed away from the border (data not shown).

Modification of AS area does not impact on proliferation or differentiation of AP

To test whether modifications of AS size influences proliferation of apical progenitors, we performed P-H3 immunostaining on *Efnb1*$^{+/-}$ explants which showed larger differences in AS size than *Efnb1*$^{-/-}$ mutants. Mitotic figures could be observed at the center of B1- patches, suggesting higher apical constriction does not prevent progenitor divisions (Fig. 6A). Quantification of P-H3+ cells revealed that the mitotic index is similar inside and outside B1- patches (Fig. 6B), despite the fact that nuclei are located more basally inside the patches (Fig. 6C, D). In addition, immunostaining of coronal sections from *Efnb1*$^{+/-}$ embryos with markers of apical (Pax6) and basal progenitors (Tbr2) showed no difference in B1+ and B1- patches (Fig.6E). Lastly, neuronal production, assessed with Ctip2 and Satb2 as markers of early born and late born neurons, respectively, is similar in B1+ and B1- patches (Fig.6E). Altogether, these results show that modifications in AS size does not correlate with changes in progenitor proliferation and/or differentiation.

DISCUSSION

Differences in apical progenitors AS sizes over the course of development or in different brain region in the mouse have been reported previously (Nagasaka and Miyata, 2021; Nishizawa et al., 2007). In addition, differences between species have been observed, for instance, AS tend to be larger in the mouse than in the ferret neocortex (Okamoto et al., 2014). However, none of these studies investigated what could be the mechanisms driving AS size changes.

Here we show that the AS of apical progenitors in the developing neocortex is heterogeneous in size ranging from 1 μm^2 to more than 20 μm^2 at mid-corticogenesis. While some of this heterogeneity comes from the modification of AS during cell division, our live imaging data indicates that it is not the sole driver of AS size heterogeneity. One possible interpretation for apical progenitors with small and others with large AS areas, is that AS size reflects the existence of different apical progenitors. Indeed, several types of apical progenitors have been described in the neocortex based on morphological features (Xing et al., 2021). For instance radial glial cells extend a basal process all the way to the pial surface of the neocortex while apical intermediate progenitors or subapical progenitors harbor a shorter basal process (Gal et al., 2006; Pilz et al., 2013). The absence of specific molecular markers for each type of apical progenitor precludes a definitive conclusion, yet, it has recently been shown in the primate neocortex that the transition from neuroepithelial cells to apical progenitors is accompanied by a decrease in AS area (Benito-Kwiecinski et al., 2021), supporting the notion that different types of neural progenitors have different morphological features including different AS sizes.

Regardless of the type of apical progenitors, how might AS size be regulated ? Here, we identified ephrin B1 as a molecular player acting on apical progenitor AS size. In *Efnb1* homozygous null embryos, the distribution of AS areas is shifted, compared to the wild type context, with a higher proportion of apical progenitors with large AS area. This is consistent with observations made in *Xenopus laevis* embryos showing that loss of ephrin B2 prevents apical constriction and leads to neural tube closure defects (Ji et al., 2014). Further, it was shown previously in sea urchin embryos that Eph:ephrin

signaling promotes apical constriction of ciliary band cells in an actomyosin-dependent manner (Krupke and Burke, 2014), revealing a potential mechanism by which ephrin B1 could control apical progenitors AS size in the mouse. However, when assessing junctional tension in *Efnb1*$^{-/-}$ tissue as a proxi for cortical actomyosin contraction, we observed an increased tension, which is not consistent with a relaxation of actomyosin-driven apical constriction. Another possible explanation for the increased AS size in *EfnB1*$^{-/-}$ explants could be that absence of ephrin B1 increases cell adhesion. It is known that adhering cells tend to spread onto a surface or increase their surface of contact with their neighbors, as was shown for E-cadherin-mediated adhesion (de Vries et al., 2004). Since Eph : Ephrin B1 signaling induces the shedding of E-cadherin via ADAM10 (Solanas et al., 2011), absence of Ephrin B1 may increase cadherin -mediated adhesion of apical progenitors AS.

Our data in *Efnb1*$^{+/-}$ tissue supports this hypothesis. Indeed, in this mosaic situation, we observe typical differential adhesion-based sorting out of Ephrin B1 positive and Ephrin B1 negative AS, and this correlates with changes in AS size. However, unexpectedly, both B1+ and B1- cells exhibit enlarged AS at patches boundary, which suggests that modification of adhesion at the B1+ / B1- boundary has non-autonomous consequences on neighboring cells. One striking non autonomous consequence is apical constriction of AS in the center of the patches, independently of the Ephrin B1 expression status within constricted cells. A similar phenotype has been reported previously for Echinoid clones in Drosophila wing disc epithelium. It was shown that Echinoid$^{+/-}$ and Echinoid$^{-/-}$ cells at clonal boundary had enlarged apical surfaces while Echinoid$^{-/-}$ cells inside the clone had reduced apical surfaces (Wei et al., 2005). In addition, when *ed* clones grew large, apical constriction disappeared. Given that Echinoid is a component of adherens juncton that cooperate with DE-cadherin in cell adhesion, these observations further suggest that ephrin B1 non autonomously modulates AS size via a role on cell adhesion.

In addition to intrinsic molecular control, mechanical cues exerted at the ventricular surface of the tissue may also contribute to the modification of apical progenitors AS area. These mechanical cues include pressure from the cerebrospinal fluid as well as physical constraints exerted laterally and/or

radially as the tissue grows through division and differentiation of neural progenitors (Abuwarda and Pathak, 2020). For instance it was recently proposed that IKNM fluidizes the neuroepithelium at early stages of development, when proliferation rates are high, while at later stages when proliferation rates decline, the tissue effectively solidifies (Bocanegra-Moreno et al., 2022). One possible role for Ephrin B1 in apical progenitors may be to provide buffering to mechanical perturbations and contribute to maintain AS area within a certain range.

At tissue level, the severe apical constriction at the center of the B1+ and B1- patches leads to an altered positioning of apical progenitors nuclei and to microfolding of the ventricular surface (Arvanitis et al., 2013). As a consequence, nuclei divide at more basal positions in B1+ and B1- patches, yet this does not change proliferation or differentiation rate, unlike what was shown in the zebrafish (Hiscock et al., 2018).

Altogether, our data reveals heterogeneity in apical progenitors AS area in the developing neocortex and shows a role for Ephrin B1 in controlling AS size. Our study also reveals that changes in AS size does not seem to have strong repercussion on apical progenitor behavior.

EXPERIMENTAL PROCEDURES

Animals

Wild-type (*Efnb1*$^{+/+}$), heterozygote female (*Efnb1*$^{+/-}$), homozygote female (*Efnb1*$^{-/-}$) and hemizygote male (*Efnb1*$^{Y/-}$) were described previously (Davy et al., 2004) and kept in a mixed 129S4/C57BL/6J genetic background. For clarity in embryonic studies, *Efnb1*$^{-/-}$ refers to *Efnb1*-null embryos of both genders. Mice were housed in the CBI animal facility. Animal procedures were approved by the appropriate Ethics committee (APAFIS#1289-2015110609133558 v5) and carried out in accordance with the European Communities Council Directive of 24 November 1986 (86/609/EEC). None of the procedures used in this study caused pain.

Cortical explant dissection and staining

Timed-pregnant *Efnb1*$^{+/-}$ mice, crossed to *Efnb1*$^{y/-}$ males, were sacrificed in a CO_2 euthanasia chamber. Embryos at embryonic day 13.5 and 14.5 were surgically removed and placed in ice-cold PBS. The embryonic brain was dissected and fixed for at least 2hrs in 4% PFA. Further dissection of the brain was performed to obtain cortical explants. Explants were then fixed in 2% PFA for an additional 2 minutes and permeabilized in PBST (PBS+0.1% Triton X100) for 10 minutes. Following a blocking step

in PBST + 5% CSF, explants were incubated with primary antibodies in the blocking buffer for 2 to 3 days. After 40 minutes washes, secondary antibodies were added in blocking buffer for 1hr at room temperature. Then, explants were gently mounted under coverslips in Mowiol, and dried over-night at 4° before imaging on the Zeiss 710 Big confocal microscope, with a 63x objective.

Antibodies

Goat α-Ephrin B1 (R&D Systems AF-473, 1/50); Rabbit α-Phospho-Histone 3 (Cell Signaling 9701, 1/200).

Explant culture

Timed-pregnant wild-type mice were sacrificed in a CO_2 euthanasia chamber. Embryos at embryonic day 14.5 were surgically removed and placed in ice-cold PBS. Cortical explants were dissected and incubated in DMEM:F2 media, supplemented with a cocktail of Penicillin/streptomycin and 100nM of SirActin in a 37°C incubator with 5% CO_2. After 3hrs incubation, explants were placed on optimized live imaging dishes and maintained under gold baskets for live imaging.

Live Imaging

For time-lapse, explants were incubated in SiR-actin (SiR F-Actin labelling 50nmol SiR-actin Kit, Sirochrome, SC001) according to the manufacturer's recommendations. Images were acquired on an inverted microscope (Leica inverted DMI8) equipped with a heating chamber (set up at 37°C, 5% CO_2 and RH 90%), a spinning disk confocal head (CSU-X1-M1N, Yokogawa) a SCMOS camera and a 63X oil immersion Plan-Apochromat objective (NA 1,4–0,7). We recorded 15 µm thick z stacks (0.5 µm z-steps) at 5min intervals (for 20hrs), with a pixel size of 120 nm (63X).

Photo-ablation

For photo-ablation, explants were treated as for live-imaging except that they were placed on small dishes with a glass bottom. Laser ablation experiments were performed using a pulsed Lined Q switch Yag double laser (532 nm, pulse length 0.4 ns, repetition rate up to 7 kHz, 7 µJ/pulse) steered by a galvanometer-based laser scanning device (Ilas2, Roper Scientific), mounted on a Leica DMI6000B inversed microscope. The laser beam was focused through an oil-immersion lens of high numerical aperture (Plan-Apochromat ×100/0.7-1.4 Imm Oil, from Leica).

Photo-ablation of apical junctions was done in the focal plane following a line of 1.6 µm for 40ms at 30% laser power (total of 10 iterations, with a thickness of 1). Live images were acquired on the wide-field microscope with a CCD HQ2 cooled Ropper cameras with a pixel size of 64.5 nm/pixel, using a Cy5 filter and HBO illumination, limiting photobleaching. Acquisition was performed every 1 second during 2 seconds, before ablation, and, every second during 10 seconds, then every 10 second during 70 seconds, after ablation. Data analysis was performed with the ImageJ software using MtrackJ Plugin.

Image analysis

Huygens, IMARIS and ImageJ software were used for image processing and data analysis.

For apical sizes measurement, actin images were first segmented using Tissue Analyzer plugin in ImageJ (Aigouy et al., 2016). Global apical areas and AS of tagged cells were calculated automatically from segmented images using the EpiTools plugin in Icy (Heller et al., 2016). AS size measurement of mitotic cell was done by manually tracing cell limits in ImageJ.

Statistical analyses

Statistical analyses, data management and graphical representations were done using R, Excel or GraphPad. Statistical analyses are indicated in the legend of each Figure.

ACKNOWLEDGEMENTS

The authors would like to thank members of the Davy team, especially Thomas Jungas for informal discussions and for insightful comments on the manuscript and Fraha Haidar for technical help. Thomas Mangeat and the Microscopy Core Facility LITC (Light Imaging Toulouse CBI) of CBI (Centre de Biologie Intégrative de Toulouse) » provided invaluable help with laser ablation experiments. The authors would like to thank the Anexplo-CBI animal facility platform for housing the mice. This work was funded by the Fondation pour la Recherche Médicale (DEQ20180339174) and by core funding from CNRS and Université Paul Sabatier.

Grant sponsor and number : This work was funded by the Fondation pour la Recherche Médicale (DEQ20180339174) and by core funding from CNRS and Université Paul Sabatier.

Author contributions: CB conceived the study, designed and performed experiments, collected and analyzed data, wrote and edited the manuscript; CA performed experiments, analyzed data and edited the manuscript; AD conceived and supervised the study, analyzed data, wrote and edited the manuscript.

Data availability: Data is available on request to the corresponding author.

Conflict of interest: The authors declare no conflict of interests.

Ethical considerations: Animal procedures were approved by the appropriate Ethics committee (APAFIS#1289-2015110609133558 v5) and carried out in accordance with the European Communities Council Directive of 24 November 1986 (86/609/EEC).

REFERENCES

Abuwarda, H., and Pathak, M.M. (2020). Mechanobiology of neural development. Current Opinion in Cell Biology *66*, 104–111. https://doi.org/10.1016/j.ceb.2020.05.012.

Aigouy, B., Umetsu, D., and Eaton, S. (2016). Segmentation and Quantitative Analysis of Epithelial Tissues. Methods Mol Biol *1478*, 227–239. https://doi.org/10.1007/978-1-4939-6371-3_13.

Arvanitis, D.N., Behar, A., Tryoen-Tóth, P., Bush, J.O., Jungas, T., Vitale, N., and Davy, A. (2013). Ephrin-B1 maintains apical adhesion of neural progenitors. Development *140*, 2082–2092. .

Benito-Kwiecinski, S., Giandomenico, S.L., Sutcliffe, M., Riis, E.S., Freire-Pritchett, P., Kelava, I., Wunderlich, S., Martin, U., Wray, G.A., McDole, K., et al. (2021). An early cell shape transition drives evolutionary expansion of the human forebrain. Cell *184*, 2084-2102.e19. https://doi.org/10.1016/j.cell.2021.02.050.

Bocanegra-Moreno, L., Singh, A., Hannezo, E., Zagorski, M., and Kicheva, A. (2022). Cell cycle dynamics controls fluidity of the developing mouse neuroepithelium. 2022.01.20.477048. https://doi.org/10.1101/2022.01.20.477048.

Cayuso, J., Xu, Q., and Wilkinson, D.G. (2015). Mechanisms of boundary formation by Eph receptor and ephrin signaling. Dev Biol https://doi.org/10.1016/j.ydbio.2014.11.013.

Compagni, A., Logan, M., Klein, R., and Adams, R.H. (2003). Control of skeletal patterning by ephrinB1-EphB interactions. Dev. Cell *5*, 217–230. .

Davy, A., Aubin, J., and Soriano, P. (2004). EphrinB1 forward and reverse signaling are required during mouse development. Genes Dev. *18*, 572–583. .

Fagotto, F., Winklbauer, R., and Rohani, N. (2014). Ephrin-Eph signaling in embryonic tissue separation. Cell Adh Migr *8*, 308–326. https://doi.org/10.4161/19336918.2014.970028.

Gal, J.S., Morozov, Y.M., Ayoub, A.E., Chatterjee, M., Rakic, P., and Haydar, T.F. (2006). Molecular and Morphological Heterogeneity of Neural Precursors in the Mouse Neocortical Proliferative Zones. J. Neurosci. *26*, 1045–1056. https://doi.org/10.1523/JNEUROSCI.4499-05.2006.

Heller, D., Hoppe, A., Restrepo, S., Gatti, L., Tournier, A.L., Tapon, N., Basler, K., and Mao, Y. (2016). EpiTools: An Open-Source Image Analysis Toolkit for Quantifying Epithelial Growth Dynamics. Dev Cell *36*, 103–116. https://doi.org/10.1016/j.devcel.2015.12.012.

Hiscock, T.W., Miesfeld, J.B., Mosaliganti, K.R., Link, B.A., and Megason, S.G. (2018). Feedback between tissue packing and neurogenesis in the zebrafish neural tube. Development *145*, dev157040. https://doi.org/10.1242/dev.157040.

Ji, Y.J., Hwang, Y.-S., Mood, K., Cho, H.-J., Lee, H.-S., Winterbottom, E., Cousin, H., and Daar, I.O. (2014). EphrinB2 affects apical constriction in Xenopus embryos and is regulated by ADAM10 and flotillin-1. Nat Commun *5*, 3516. https://doi.org/10.1038/ncomms4516.

Krupke, O.A., and Burke, R.D. (2014). Eph-Ephrin signaling and focal adhesion kinase regulate actomyosin-dependent apical constriction of ciliary band cells. Development *141*, 1075–1084. https://doi.org/10.1242/dev.100123.

Martin, A.C., Kaschube, M., and Wieschaus, E.F. (2009). Pulsed contractions of an actin-myosin network drive apical constriction. Nature *457*, 495–499. https://doi.org/10.1038/nature07522.

Miyata, T., Kawaguchi, A., Saito, K., Kawano, M., Muto, T., and Ogawa, M. (2004). Asymmetric production of surface-dividing and non-surface-dividing cortical progenitor cells. Development *131*, 3133–3145. https://doi.org/10.1242/dev.01173.

Nagasaka, A., and Miyata, T. (2021). Comparison of the Mechanical Properties Between the Convex and Concave Inner/Apical Surfaces of the Developing Cerebrum. Front Cell Dev Biol *9*, 702068. https://doi.org/10.3389/fcell.2021.702068.

Nagele, R.G., and Lee, H.Y. (1979). Ultrastructural changes in cells associated with interkinetic nuclear migration in the developing chick neuroepithelium. J Exp Zool *210*, 89–106. https://doi.org/10.1002/jez.1402100110.

Nishizawa, Y., Imafuku, H., Saito, K., Kanda, R., Kimura, M., Minobe, S., Miyazaki, F., Kawakatsu, S., Masaoka, M., Ogawa, M., et al. (2007). Survey of the morphogenetic dynamics of the ventricular surface of the developing mouse neocortex. Dev Dyn *236*, 3061–3070. https://doi.org/10.1002/dvdy.21351.

Noctor, S.C., Martinez-Cerdeno, V., Ivic, L., and Kriegstein, A.R. (2004). Cortical neurons arise in symmetric and asymmetric division zones and migrate through specific phases. Nat Neurosci *7*, 136–144. https://doi.org/10.1038/nn1172.

Okamoto, M., Shinoda, T., Kawaue, T., Nagasaka, A., and Miyata, T. (2014). Ferret-mouse differences in interkinetic nuclear migration and cellular densification in the neocortical ventricular zone. Neurosci Res *86*, 88–95. https://doi.org/10.1016/j.neures.2014.10.006.

Pilz, G.-A., Shitamukai, A., Reillo, I., Pacary, E., Schwausch, J., Stahl, R., Ninkovic, J., Snippert, H.J., Clevers, H., Godinho, L., et al. (2013). Amplification of progenitors in the mammalian telencephalon includes a new radial glial cell type. Nat Commun *4*, 2125. https://doi.org/10.1038/ncomms3125.

Pinheiro, D., and Bellaïche, Y. (2018). Mechanical Force-Driven Adherens Junction Remodeling and Epithelial Dynamics. Dev Cell *47*, 3–19. https://doi.org/10.1016/j.devcel.2018.09.014.

Sauer, M.E., and Walker, B.E. (1959). Radioautographic Study of Interkinetic Nuclear Migration in the Neural Tube. Proceedings of the Society for Experimental Biology and Medicine *101*, 557–560. https://doi.org/10.3181/00379727-101-25014.

Sawyer, J.M., Harrell, J.R., Shemer, G., Sullivan-Brown, J., Roh-Johnson, M., and Goldstein, B. (2010). Apical constriction: a cell shape change that can drive morphogenesis. Dev Biol *341*, 5–19. https://doi.org/10.1016/j.ydbio.2009.09.009.

Solanas, G., Cortina, C., Sevillano, M., and Batlle, E. (2011). Cleavage of E-cadherin by ADAM10 mediates epithelial cell sorting downstream of EphB signalling. Nat Cell Biol *13*, 1100–1107. https://doi.org/10.1038/ncb2298.

Tyler, S. (2003). Epithelium—The Primary Building Block for Metazoan Complexity1. Integrative and Comparative Biology *43*, 55–63. https://doi.org/10.1093/icb/43.1.55.

de Vries, W.N., Evsikov, A.V., Haac, B.E., Fancher, K.S., Holbrook, A.E., Kemler, R., Solter, D., and Knowles, B.B. (2004). Maternal β-catenin and E-cadherin in mouse development. Development *131*, 4435–4445. https://doi.org/10.1242/dev.01316.

Wei, S.-Y., Escudero, L.M., Yu, F., Chang, L.-H., Chen, L.-Y., Ho, Y.-H., Lin, C.-M., Chou, C.-S., Chia, W., Modolell, J., et al. (2005). Echinoid is a component of adherens junctions that cooperates with DE-Cadherin to mediate cell adhesion. Dev Cell *8*, 493–504. https://doi.org/10.1016/j.devcel.2005.03.015.

Xing, L., Wilsch-Bräuninger, M., and Huttner, W.B. (2021). How neural stem cells contribute to neocortex development. Biochem Soc Trans BST20200923. https://doi.org/10.1042/BST20200923.

FIGURE LEGENDS

Figure 1. AS of apical progenitors is heterogeneous in size.

A. Schematic representation of the dissection procedure to visualize the AS of apical progenitors in an 'En-Face' view.

B. En-Face view of an E13.5 cortical slab stained for actin (left) and color-coded from light blue (0 μm^2) to dark red (23 μm^2), as calculated after segmentation (right). Scale bar= 10 μm.

C. Distribution of AS areas, measured from 5 different embryos at E13.5 (2-3 images for each cortex, >200000 cells total). Error bars indicate SEM. Average 4.4 μm^2 +/- 0.21 – Median 3.8 μm^2.

D. AS sizes at E13.5 compared to E14.5 and E14.5 + 14Hrs. Data represents average +/- SEM. Unpaired t-test *p<0,05; **p<0,01.

E. Apical view of a E14.5 cortical slab stained for actin, before (T0) and after 14 hours in culture (E14.5 + 14Hrs). Scale bar= 10 μm.

F. Distribution of AS sizes, averages from 3 different E14.5 cortical explants in culture (3 images for each, >3000 cells total). Data represents average +/- SEM.

Figure 2. Heterogeneity in AS size is not due to cell cycle phases.

A. En-Face view of a E14.5 cortical slab cultured for 15 hours with an actin dye (SirActin). Images represent 4 different times from Movie 2.

B. Zoom-in from A (white dashed region) with the skeleton superposed (red). Tagged AS (green) were followed throughout the timelaps (Movie 4).

C. Graphical representation of AS areas of 54 cells over the 15 hours movie.

D. Average change in AS area from the same cells than in C, throughout the movie. Error bars indicate SD.

E. Still images from Movie 5 with AS of a dividing apical progenitor highlighted in yellow. T0 corresponds to the time at which 2 AS were first observed after completion of cytokinesis.

F. Measurement of AS area of 22 dividing apical progenitors before and after division. T0 corresponds to the time at which 2 AS were first observed after completion of cytokinesis.

Figure 3. The distribution of apical progenitors AS size is modified in *Efnb1* mutants.

A. Laser ablation experiments on apical surfaces of cortical explants at E14.5 (Movies 6 and 7). Laser pulses (white arrows) were applied in the mid-point between two polygonal apices and junctional actin was visualized using SirActin. Scale bar= 5 μm.

B. The distance between the two separated apices (recoil) was measured for 80 seconds after laser ablation. Means +/- SEM; fitted non linear curve is shown. Average Initial recoil is higher in *Efnb1*$^{-/-}$ (0,045 -95% CI 0,035-0,059) than in *Efnb1*$^{+/+}$ (0,022 -95% CI 0,018-0,027) tissues.

C. 60 seconds post ablation, average recoil is higher in *Efnb1*$^{-/-}$ than in *Efnb1*$^{+/+}$ tissues. Each dot represents one ablated junction. n=45 in *Efnb1*$^{-/-}$ tissue and n=62 in *Efnb1*$^{+/+}$ tissue, 3 independent experiments for each genotype. Unpaired t test, p<0,0001.

D. En-Face view of cortical explants from E13.5 *Efnb1*$^{+/+}$, *Efnb1*$^{+/-}$ and *Efnb1*$^{-/-}$ embryos stained for actin. Scale bar= 10 μm.

E. Color-coded representations of AS areas in the 3 genotypes, calculated after segmentation (different images than in D), from light blue (0 μm^2) to dark red (23 μm^2). Scale bar= 10 μm.

F. Average AS area for each genotype. Error bars indicate SEM.

G. Distribution of AS sizes, averages from at least 4 different embryos per genotype at E13.5 (2-3 images for each cortex, 167096 cells total). Error bars indicate SD.

H. Distribution of AS sizes in *Efnb1*$^{+/-}$ and *Efnb1*$^{-/-}$ mutants in ratio compared to the WT (set at 1). Polynomial trend lines are shown for both *Efnb1* mutants.

Figure 4. Modification of AS size in *EfnB1*$^{+/-}$ mosaic contexts.

A. Coronal section of E13.5 *Efnb1*$^{+/-}$ brain stained for Ephrin B1 (green) and DNA (blue), Scale bar = 500 μm.

B. Apical view of *Efnb1*$^{+/-}$ cortex, at E13.5 (left) and E14.5 (right), stained for actin (grey) and Ephrin B1 (green). A drawing of some cells was superimposed on the actin staining (bottom), with a color code to show the different layers of cells at the boundary of Ephrin B1- patches (B1- cells in red and B1+ cells in green). Scale bar=20μm.

C, D. Average sizes of AS relative to their rank from the cluster boundary at E13.5 (C) and E14.5 (D). Measurements were done for 3 clusters at E13.5 and 6 at E14.5, data are showing averages +/- SEM. Sydak's multiple comparisons test, adjusted P-values **** p<0.0001, *** p<0.001, ** p<0.01.

E. Schematic representation of cell layers at the boundary of Ephrin B1- patches with the layers numbered as in C and D.

F. Apical view of *Efnb1*$^{+/-}$ cortex, stained for actin (grey) and Ephrin B1 (green), Z reconstructions are shown below the X/Y images, at the level indicated by the white dashed line. Scale bar=20μm

Figure 5. The modification of AS size in *EfnB1*$^{+/-}$ mosaic contexts is not cell autonomous.

A. Apical view of *Efnb1*$^{+/-}$ cortex at E13.5 stained for actin (grey) and Ephrin B1 (green). A drawing of some cells was superimposed on the actin staining (right), with a color code to show the different

layers of cells at the boundary of the Ephrin B1+ patch (B1+ cells in red and B1- cells in green). Scale bar=10μm.

B. Average sizes of AS relative to their rank from the cluster boundary. Measurement were done for 3 clusters, data are showing averages +/- SEM. Sydak's multiple comparisons test, adjusted P-values **** p<0.0001, * p<0.05.

C. Schematic representation of cell layers at the boundary of Ephrin B1 positive clusters with the layers numbered as in B.

Figure 6. Modification of AS size does not impact proliferation or differentiation of apical progenitors.

A. En-face view of *Efnb1*$^{+/-}$ cortex at the level of mitotic nuclei. Cortical slabs were stained for DNA (blue), actin (grey), Phospho-Histone H3 (P-H3, red) and Ephrin B1 (green). Scale bar=10μm.

B. Percentage of P-H3+ nuclei in Ephrin B1 negative and Ephrin B1 positive territories. Quantification was done on 2684 B1- and 5115 B1+ cells from at least 3 different clusters. Data are showing averages +/- SD.

C. Apical view of *Efnb1*$^{+/-}$ cortex, stained for actin (grey) and Ephrin B1 (green), Z reconstructions are shown below the X/Y images, at the cut indicated by a red dashed line. Scale bar=10μm.

D. Quantification of the distance between nuclei and the apical surface in B1+ and B1- territories. Each dot is a nucleus.

E. Coronal sections of E14.5 *Efnb1*$^{+/-}$ cortex stained for Pax6, Tbr2, Ctip2 or Satb2, as indicated. Nuclei are stained with DAPI. Scale bar=100μm

Figure 1.

A

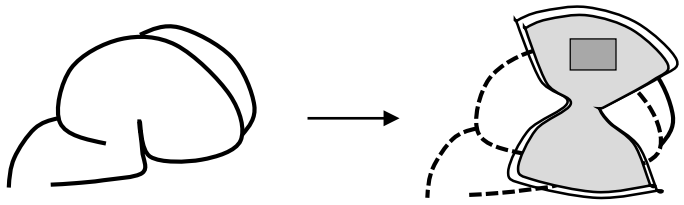

B

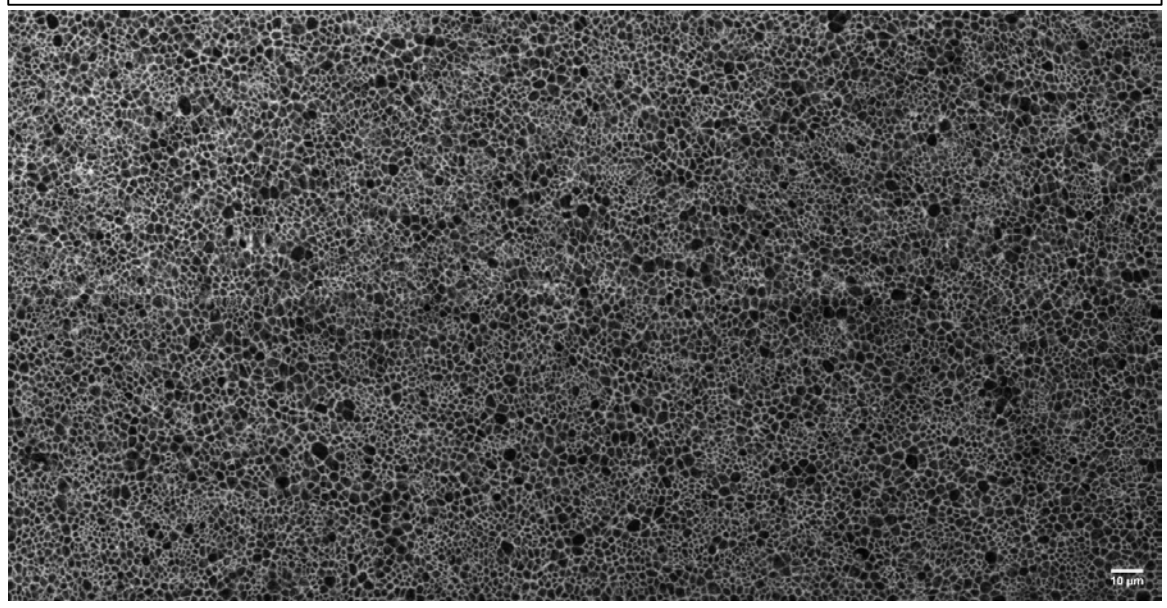

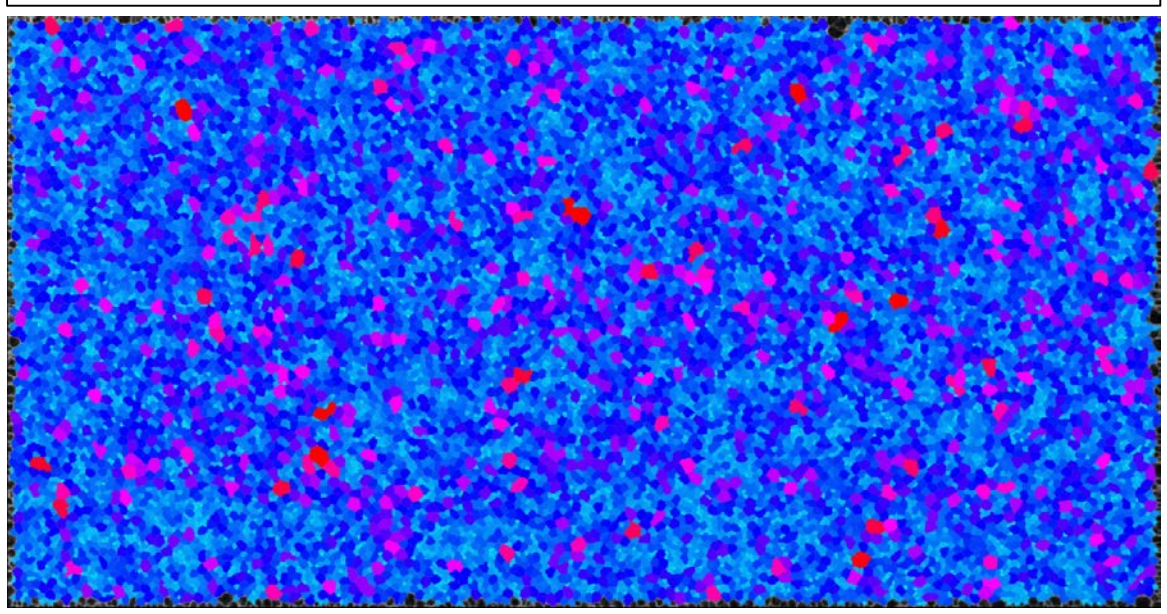

C

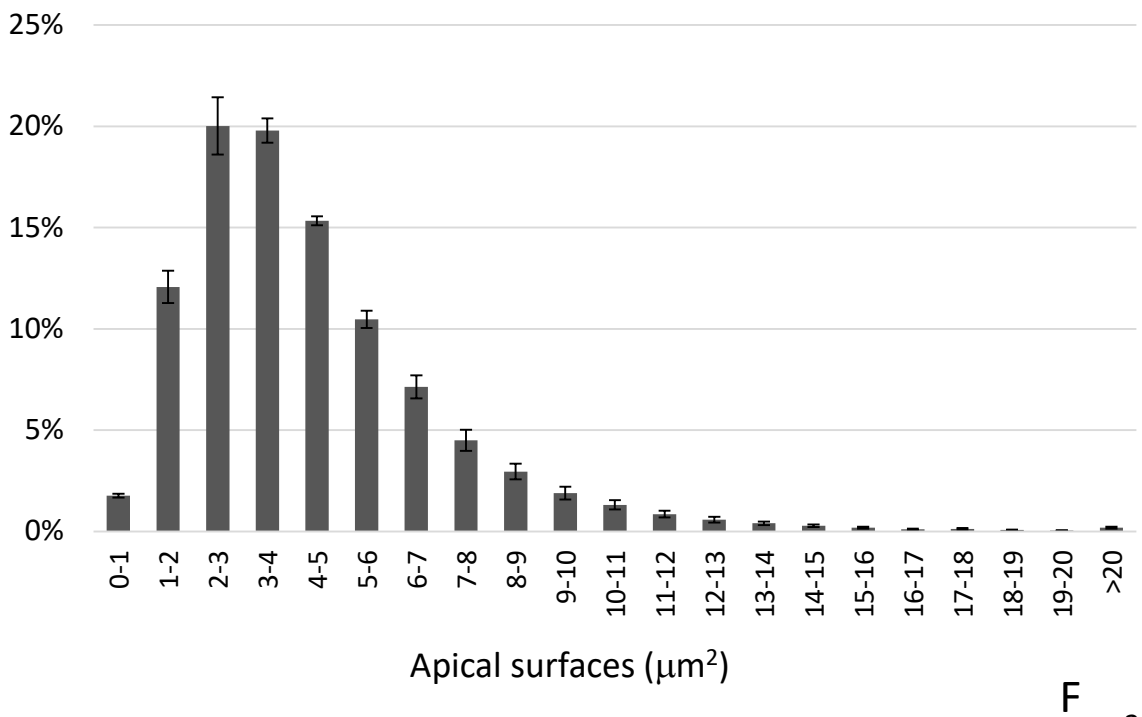

D

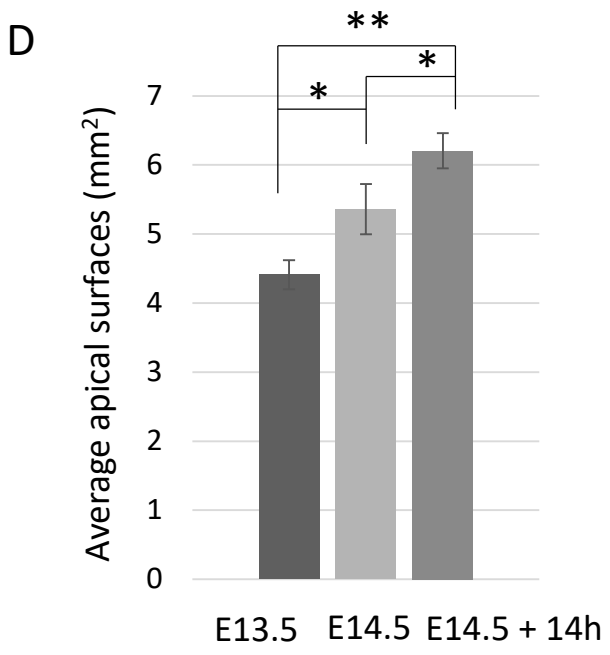

E

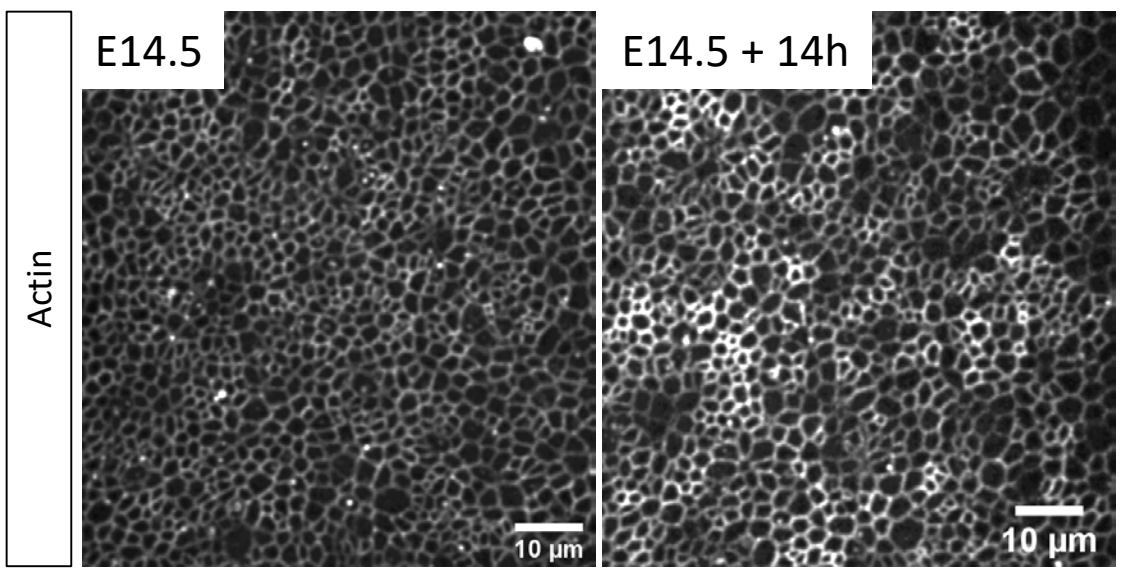

F

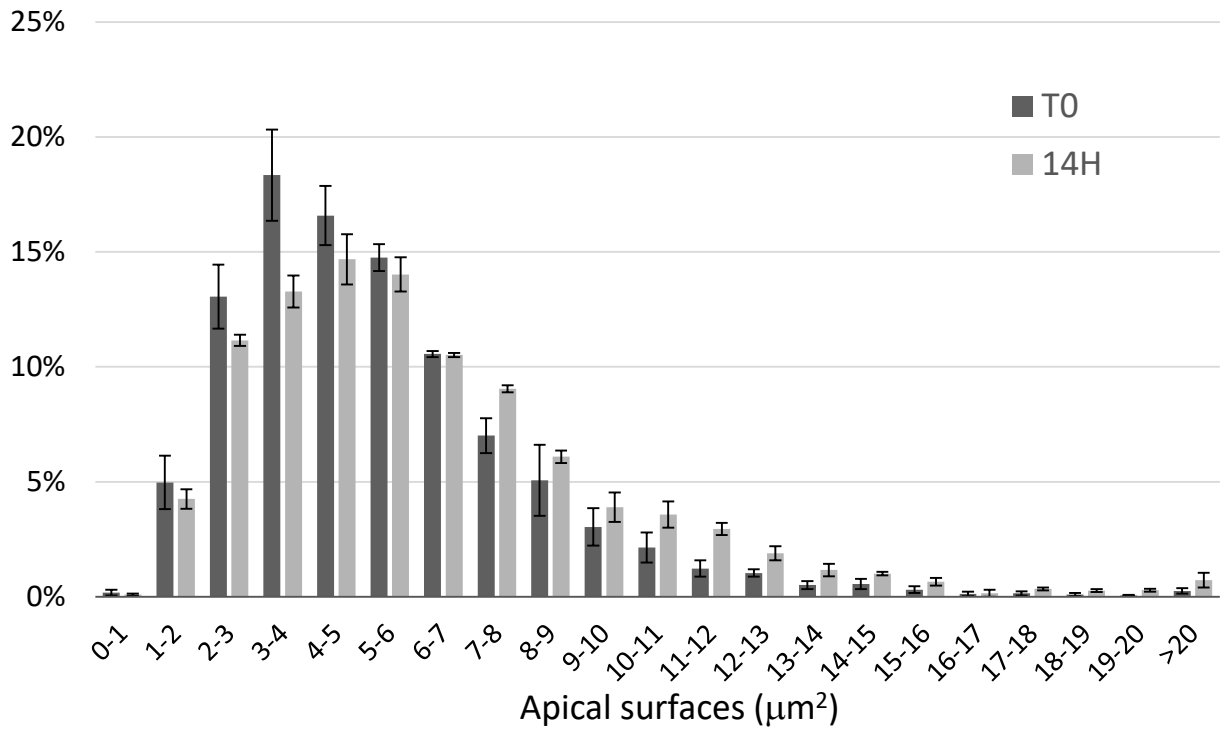

Figure 2.

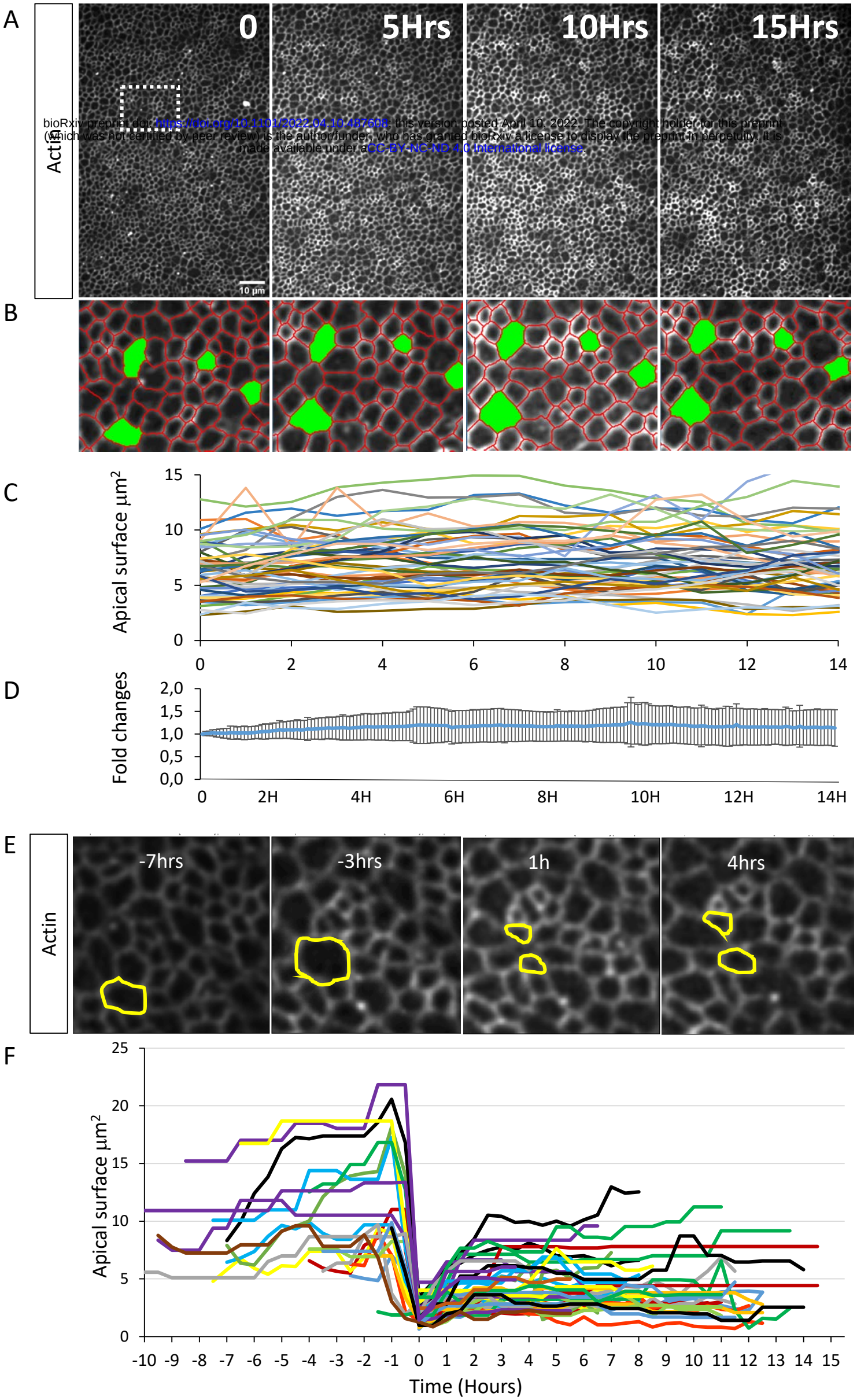

Figure 3.

Figure 4.

A

Efnb1$^{+/-}$

Ephrin B1 / DNA

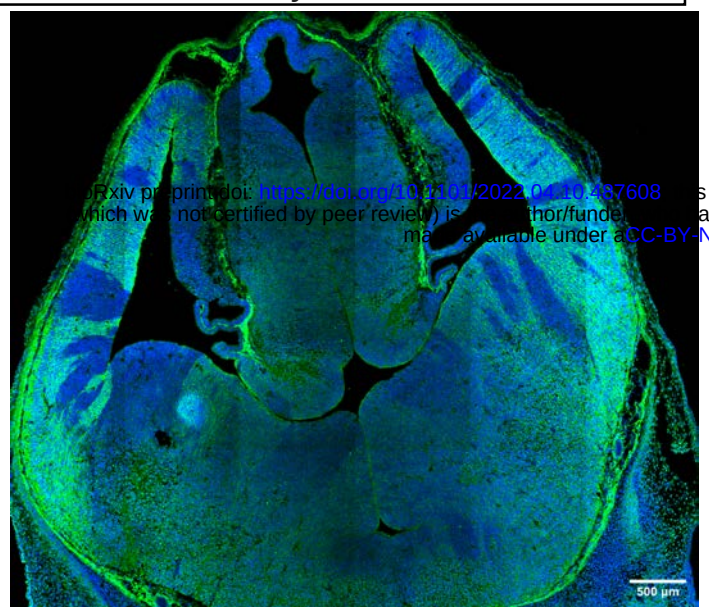

B

E13.5

E14.5

Ephrin B1 / Actin

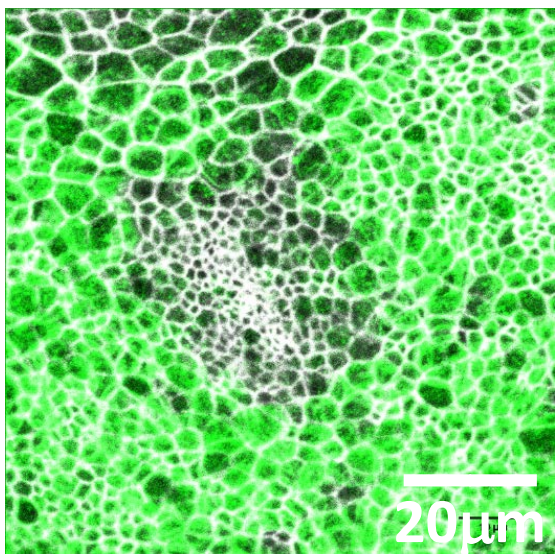

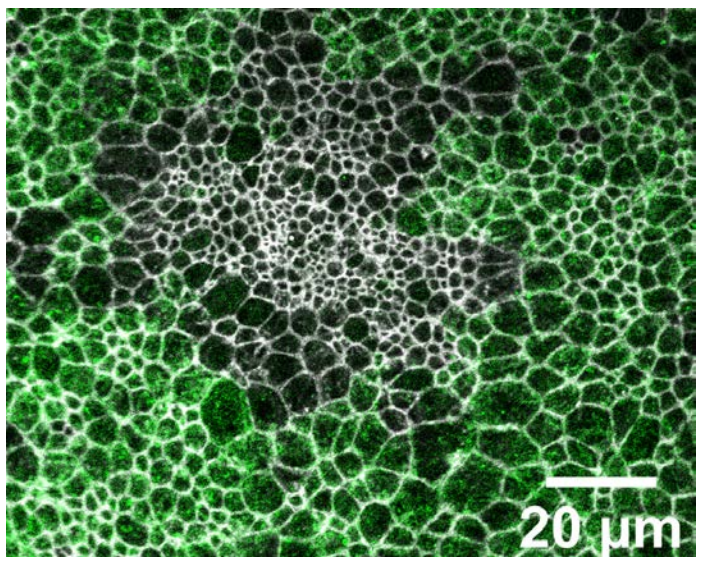

Actin

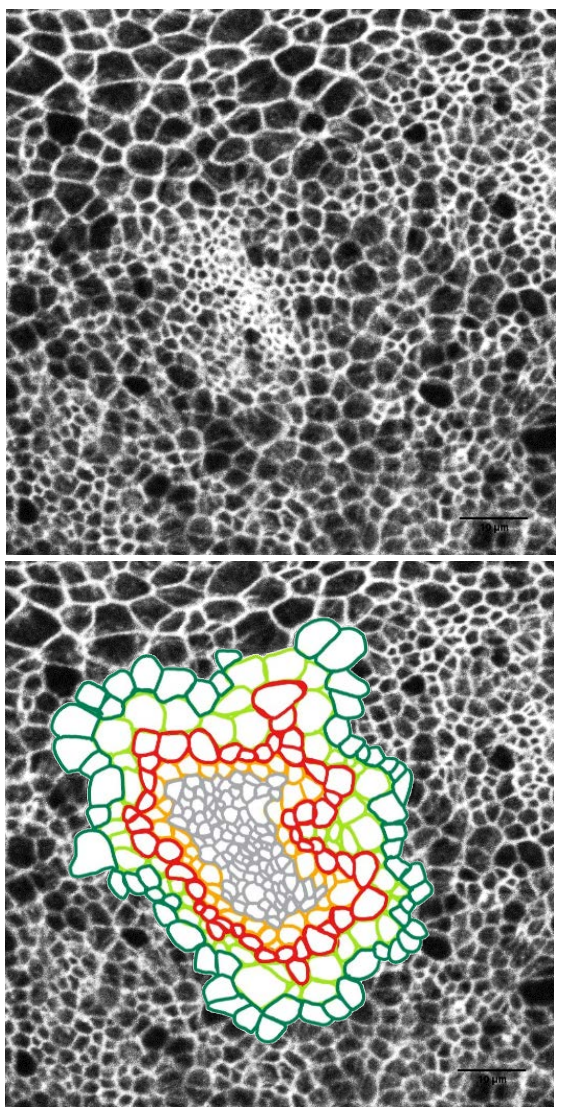

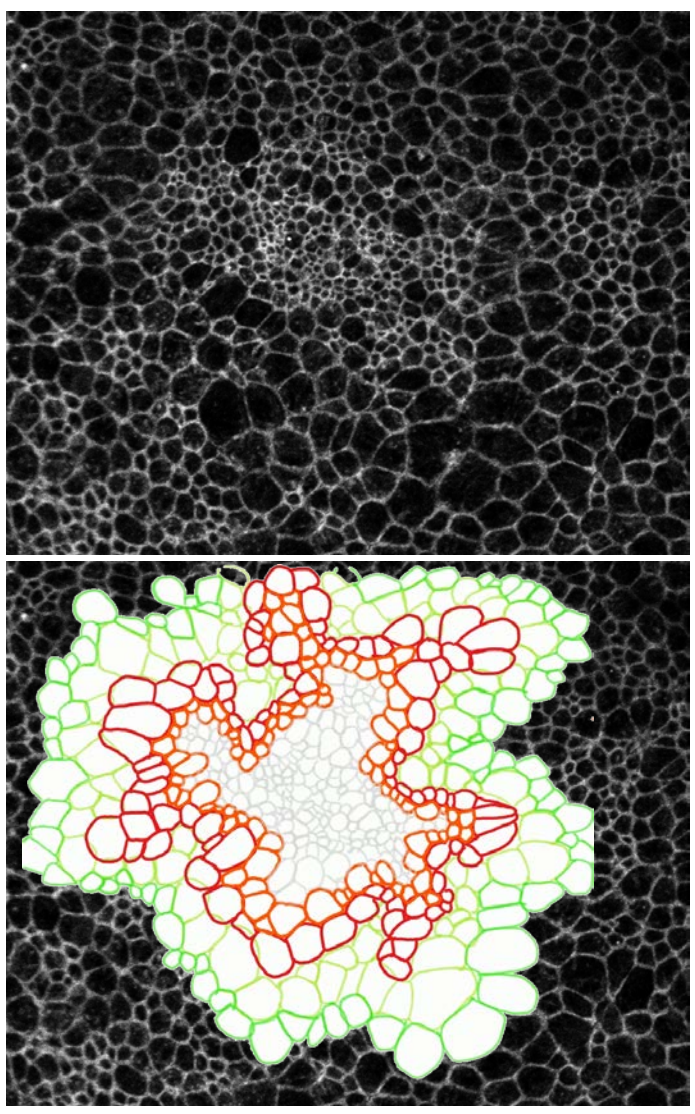

C

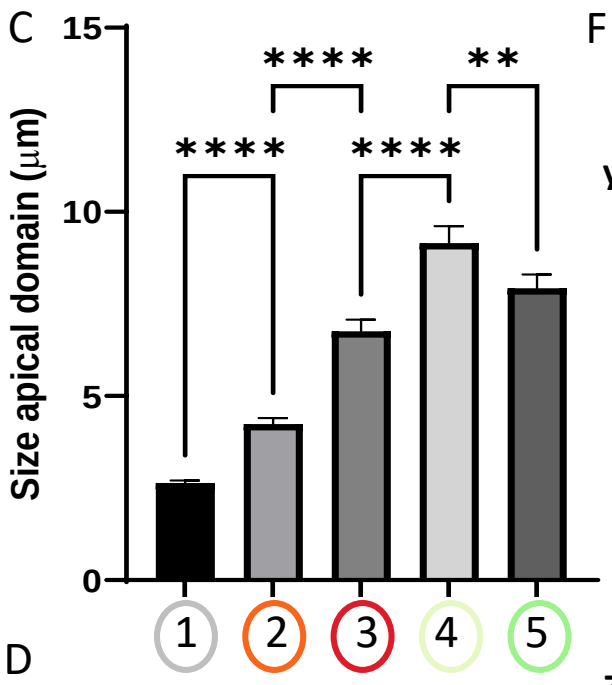

D

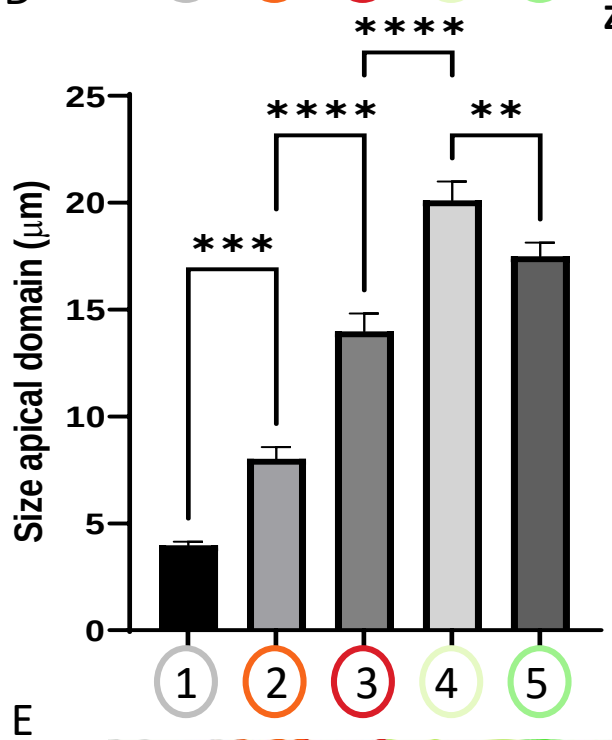

E

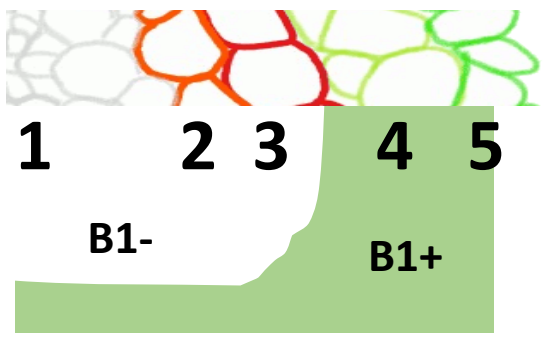

F

Ephrin B1 / Actin

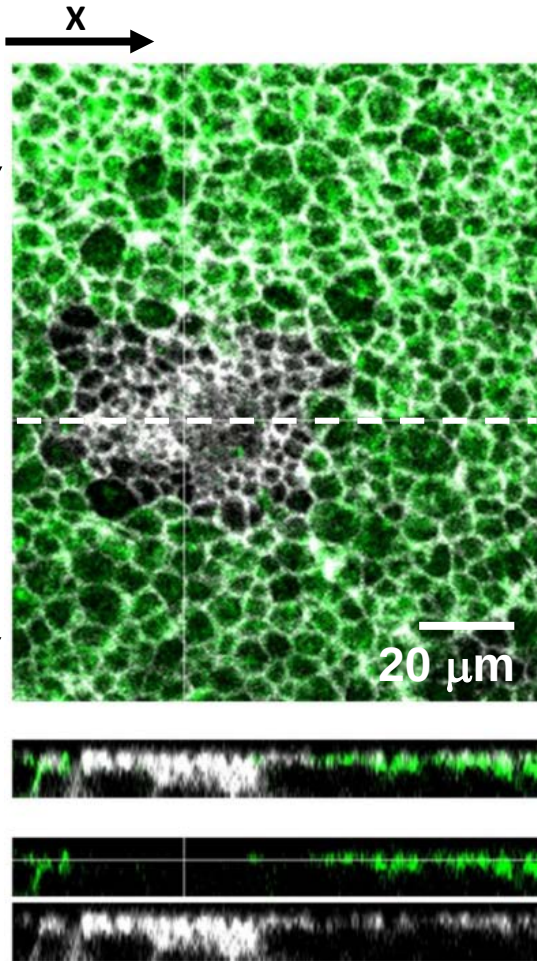

Figure 5.

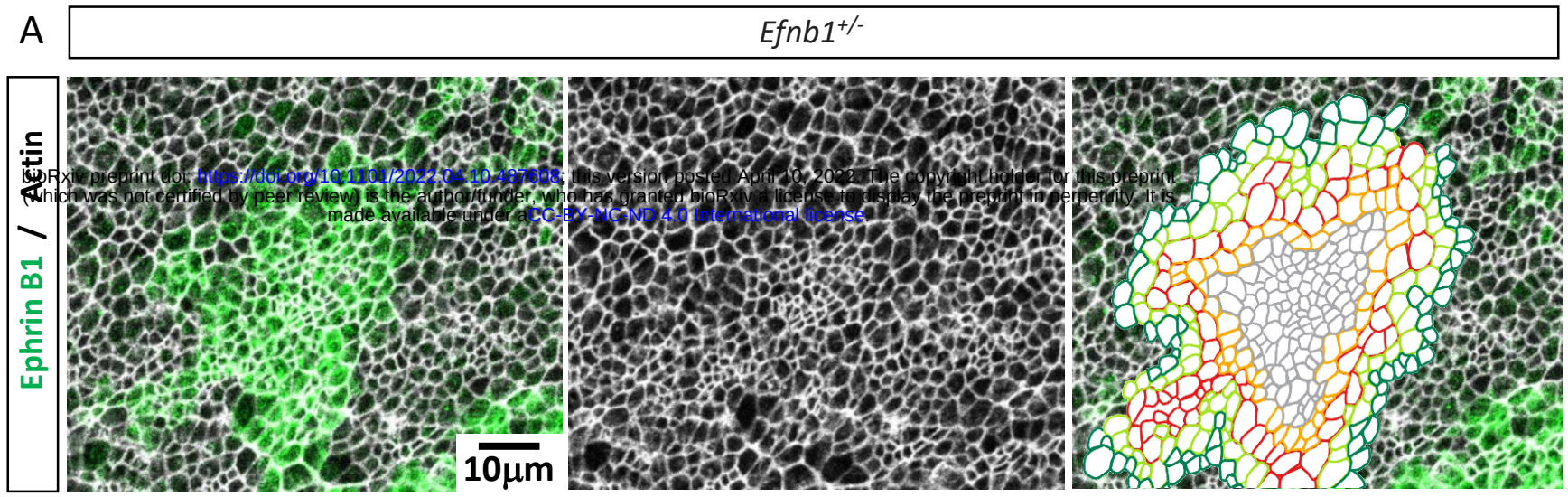

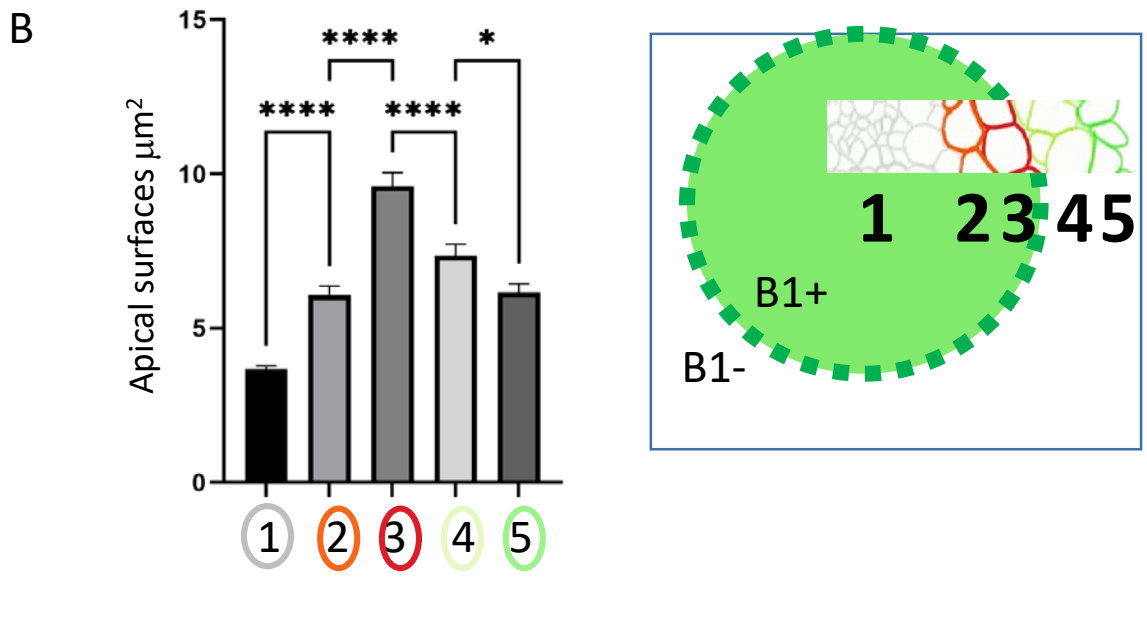

Figure 6.

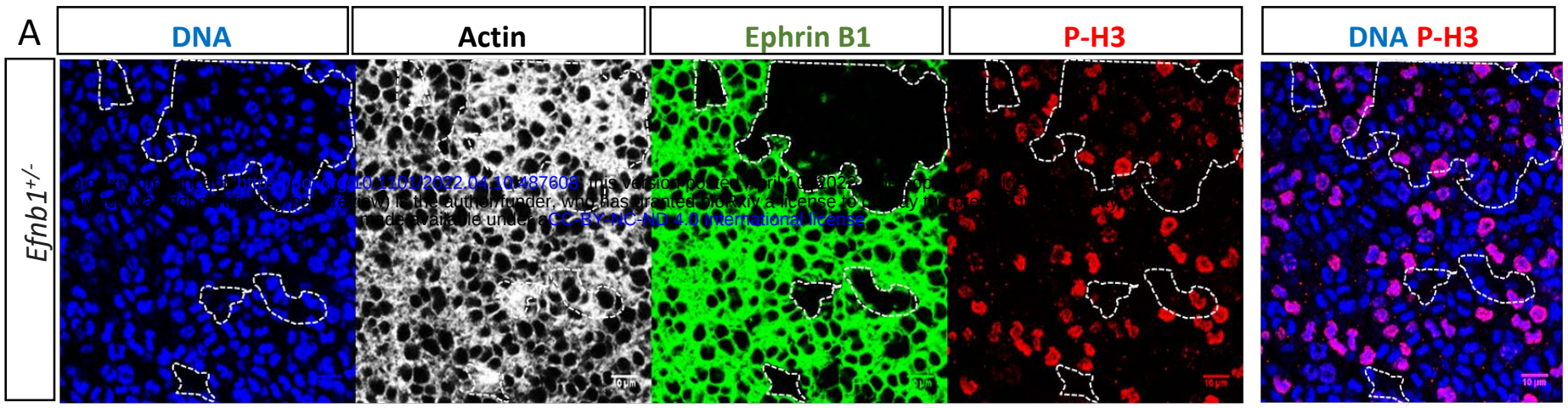
A
DNA
Actin
Ephrin B1
P-H3
DNA P-H3
Efnb1+/-

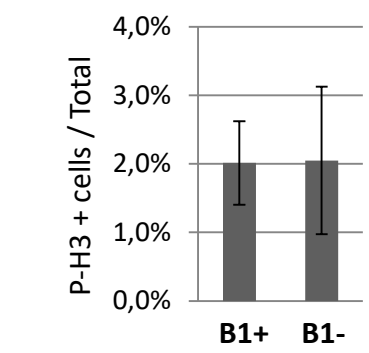
B
P-H3 + cells / Total
4,0%
3,0%
2,0%
1,0%
0,0%
B1+
B1-

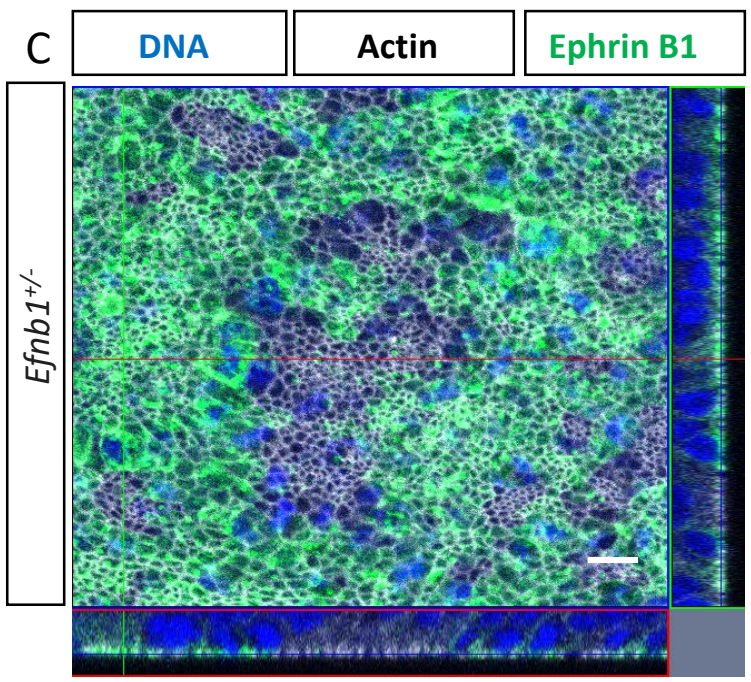
C
DNA
Actin
Ephrin B1
Efnb1+/-

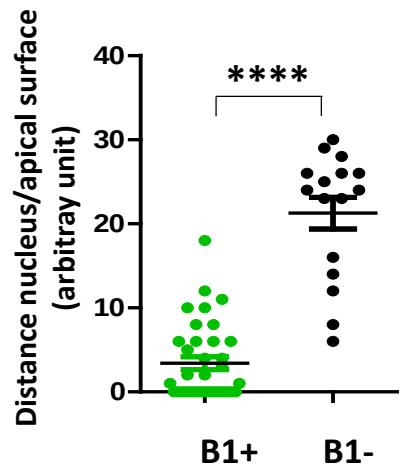
D
Distance nucleus/apical surface (arbitray unit)
40
30
20
10
0
****
B1+
B1-

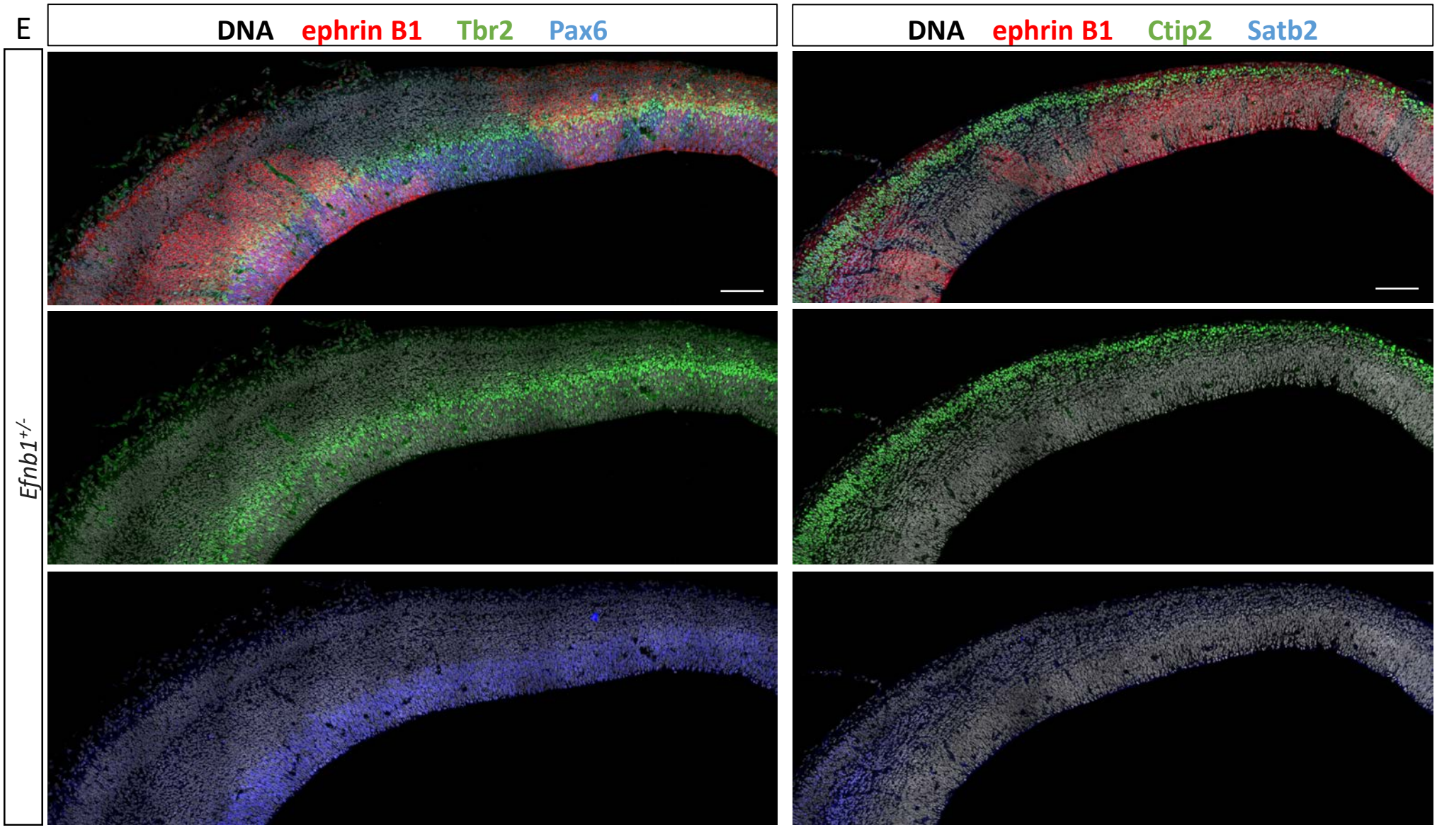
E
DNA ephrin B1 Tbr2 Pax6
DNA ephrin B1 Ctip2 Satb2
Efnb1+/-